Energy-exchange characteristics in ordinary and nonlinear Compton scattering

J. X. Wang[1] and Y. K. Ho[2,1*]
[1]*Institute of Modern Physics, Fudan University, Shanghai 200433, China*
[2]*CCAST (World Laboratory), P.O. Box 8730, Beijing 100080, China*
(Received 10 April 1998; revised manuscript received 24 September 1998)

Free-electron–photon interaction, if it occurs inside an intense laser field, will be dominated by nonlinear Compton scattering (NLCS), which is quite different from the ordinary Compton scattering. The difference can be, for example, in the number of photons involved in one interaction. In this paper, by both analytical and numerical methods, we will explore in detail their characteristics from the viewpoint of energy exchange in the interaction. Based upon the well-displayed results, we are able to, furthermore, reveal some phenomena underlying NLCS and investigate the corresponding physical implications, such as the threshold effects in NLCS. That is, when $Q=eE/(m_e\omega c)>0.1$, the low-order NLCS will be depressed while the high orders will be excited. And when $Q>10$, the high-order NLCS process will become dominant in the electron-photon interaction. As for $Q>100$, the extra-high-order NLCS will be so strongly excited that the electron dynamics will enter a new regime. Also, we can make use of the obtained results to explain qualitatively the NLCS experiment by Bula *et al.* [Phys. Rev. Lett. **76**, 3116 (1996)]. [S1050-2947(99)02106-X]

PACS number(s): 34.80.Qb, 32.80.Cy, 42.50.Vk, 41.75.−i

I. INTRODUCTION

With the advances of laser technology in the 1960s, there emerged a lot of related research areas in fundamental physics, such as multiphoton ionization [1–3], high-harmonic generation in atomic physics [4], laser-plasma interaction [5,6], laser acceleration [7], etc. Among them, the nonlinear phenomenon in the interaction of free electrons with intense laser fields in vacuum has been attracting wide attention ever since its beginning. A great deal of theoretical work in both quantum and classical frames has appeared [8–11]. Unlike atom-laser or plasma-laser interaction, to distinguish the nonlinear effect in free-electron–laser interaction, much higher intensity is needed [$I\lambda^2>10^{18}$ (W/cm^2)μm^2, where I is the laser intensity in units of W/cm^2 and λ is the wavelength in units of μm]. This nonlinear effect, usually referred to as nonlinear Compton scattering [12,13], is the process in which an electron absorbs more than one photon before a high-frequency photon is emitted. Because of this complexity, experimental research progressed very slowly until recently when Bula *et al.* succeeded in observing the absorption of up to four photons simultaneously by an electron in an interaction inside a laser field with $Q=0.6$ [14]. As usual, the laser intensity is measured by the dimensionless parameters $Q=e\sqrt{\langle A^2\rangle}/m_e=e\sqrt{\langle A^\mu A_\mu\rangle}/m_e$, in which $-e$ and m_e are the electron charge and rest mass, respectively, A^μ is the four-vector potential, and $\langle\,\rangle$ denotes the time average. Throughout this paper, we use the metric $g^{\mu\nu}=(1,-1,-1,-1)$ and the natural units with $\hbar=c=1$. The scalar product of four vectors are written simply as $a\cdot b=a^\mu b_\mu$ and $a\cdot a=a^\mu a_\mu=a^2$.

In our previous work [15–17], we have found that an electron can exchange not only momentum but also energy with a stationary intense laser beam when the field intensity meets the requirement $Q>0.1$ in the interaction region. This kind of inelastic effect originates from the nonlinear Compton scattering and provides us with more accessible standpoint to study the free-electron–intense-laser field interaction, since the charged electron can be more easily controlled in the experiments than the emitted neutral photons of weak intensity. We know that the electron energy change through the scattering is an overall effect of combined ordinary and nonlinear Compton scattering. To fully understand this inelastic effect, it is necessary to study at first in detail the characteristics of electron-photon energy exchange in both the ordinary and nonlinear Compton scattering.

At present, the chirped pulsed amplification technique developed in the 1980s has been widely applied in strong laser physics and lasers with $Q>1$ [$I\lambda^2>10^{18}$ (W/cm^2) μm^2] are readily available. As shown above, under such intense laser fields, the electron-photon interactions have entered the NLCS regime. To our knowledge, no detailed quantitative study of NLCS has ever been presented in the literature. Thus to probe NLCS and to investigate its application to strong-field effects are meaningful, which is the main motivation in carrying out the research in this paper.

In the following, we will first study the ordinary Compton scattering. Next, the focus is set on the nonlinear Compton scattering and the application to the electron inelastic scattering by an intense stationary laser beam together with the experiments. Finally, we will summarize our results.

II. ORDINARY COMPTON SCATTERING

To facilitate the discussion, we will present the theoretical formulas for ordinary Compton scattering before giving the numerical results and discussion.

A. Theory

The configuration of the following electron-photon interaction is presented in Fig. 1:

*Author to whom correspondence should be addressed. Address correspondence to Institute of Modern Physics, Fudan University, Shanghai 200433, China. FAX: +86-21-65104949. Electronic address: hoyk@fudan.ac.cn

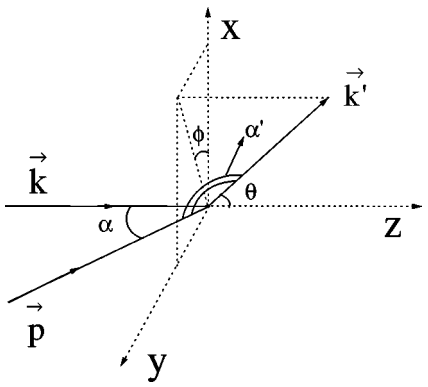

FIG. 1. The configuration of the photon–free-electron interaction. The initial photon **k** propagates along the z axis making a crossing angle α with the electron running in the direction **p**. The scattered photon $\mathbf{k}'$ is emitted to the direction defined by (θ,ϕ). The crossing angle between $\mathbf{k}'$ and **p** is α'. **p** lies in the x-z plane.

$$e+k\rightarrow e'+k'. \tag{1}$$

By standard perturbative method, the covariant differential cross section can be obtained [18]:

$$\frac{d\sigma}{dy}=\frac{2\pi r_0^2}{x}\left[\frac{4y^2}{x^2(1-y)^2}-\frac{4y}{x(1-y)}+1-y+1+\frac{1}{1-y}\right], \tag{2}$$

where $r_0=e^2/(4\pi m_e)$ is the electron classical radius,

$$y=\frac{k\cdot k'}{p\cdot k} \quad \text{and} \quad x=\frac{2p\cdot k}{m_e^2}, \tag{3}$$

in which k and k' are the photon initial and final four momentum, respectively, and p is the electron initial four momentum. The total cross section is

$$\begin{aligned}\sigma_T&=\int_0^{x/(1+x)}\frac{d\sigma}{dy}dy\\&=\frac{2\pi r_0^2}{x^2}\left[\left(1-\frac{4}{x}-\frac{8}{x^2}\right)\ln(1+x)\right.\\&\quad\left.+\frac{1}{2}+\frac{8}{x}-\frac{1}{2(1+x)^2}\right].\end{aligned} \tag{4}$$

According to the four momentum conservation,

$$p+k=p'+k', \tag{5}$$

we obtain the electron energy difference before and after the interaction,

$$\frac{\Delta E}{\omega}=\frac{\gamma\beta(\cos\alpha-\cos\alpha')+\omega/m_e(1-\cos\theta)}{\gamma(1-\beta\cos\alpha')+\omega/m_e(1-\cos\theta)}, \tag{6}$$

where α and α' are the crossing angles between the incident electron and the incident photon, between the incident electron and the emitted photon, respectively; and θ is the crossing angle between the incident and emitted photon $(0\leqslant\alpha',\theta\leqslant\pi)$. By introducing the azimuthal angle ϕ between the planes of $\mathbf{k}\times\mathbf{p}$ and $\mathbf{k}\times\mathbf{k}'$, we have

$$\cos\alpha'=\sin\alpha\sin\theta\cos\phi+\cos\alpha\cos\theta. \tag{7}$$

In the electron's rest frame, $p=(1,0,0,0)m_e$ and the interaction is independent of ϕ, which leads to

$$\pi x\,dy=\left(\frac{\omega'}{m_e}\right)^2\sin\theta\,d\theta\,d\phi=\left(\frac{\omega'}{m_e}\right)^2 d\Omega', \tag{8}$$

where $d\Omega'$ is the solid angle of the final photon. Since dy and $\omega'^2\,d\Omega'$ are Lorentz invariant, we can obtain the differential cross section in the laboratory frame,

$$\frac{d\sigma}{d\Omega'}=\frac{1}{\pi x}\left(\frac{\omega'}{m_e}\right)^2\frac{d\sigma}{dy}. \tag{9}$$

By multiplying ΔE and integrating over the solid angle $d\Omega'$, we can get the average energy change of the electron in one interaction,

$$\left(\frac{\Delta E}{\omega}\right)_{\text{ave}}=\frac{\int(d\sigma/d\Omega')(\Delta E/\omega)d\Omega'}{\sigma_T}, \tag{10}$$

which can be numerically calculated.

B. Numerical results and discussion

The practical background of our discussion is the electron interaction with an intense laser beam. Considering the usual experimental setup, in all the following analysis, we will use the optical wavelength $\lambda=1.06$ μm as an example, which leads to $\omega/m_e\approx10^{-6}$.

Usually, in order to overcome the repulsive ponderomotive potential [19] of the laser field with $Q\sim1$ to reach the beam center, the electron momentum should be at least of m_e magnitude, which means $\gamma\beta\geqslant1\gg\omega/m_e$. Thus, to the first-order approximation, we can neglect $\omega/m_e(1-\cos\theta)$ in Eq. (6), and it yields

$$\frac{\Delta E}{\omega}\approx\frac{\gamma\beta(\cos\alpha-\cos\alpha')}{\gamma(1-\beta\cos\alpha')+\omega/m_e(1-\cos\theta)}. \tag{11}$$

The above equation tells us that only when $\alpha'<\alpha$, namely, the photon is scattered into a cone around **p** with a crossing angle $\alpha_0'=\alpha$, will the electron energy be reduced after the interaction. Otherwise, the electron energy will increase. And, when the small contribution of $\omega/m_e(1-\cos\theta)$ in Eq. (6) is included, the delimiting angle α_0' will be a little smaller than α. Hence, when the electron runs along the photon propagation direction with $\alpha=0$, α_0' equals zero, too, which means the electron will never lose energy. Of course, this conclusion concerning $\alpha=0$ is generally correct and not limited by the conditions $\gamma\beta\geqslant1\gg\omega/m_e$, as can also be directly seen from Eq. (6).

Because the interaction probability is dependent on the photon scattering direction, which is of no interest to the electron inelastic scattering, the more important task next is to obtain the electron energy change averaged over the solid angle of the emitted photons. This can only be accomplished through the numerical calculations of Eq. (10).

Figures 2 and 3 show the case when $\alpha=0$. It is obvious that the electron dynamics is symmetric with respect to the azimuthal angle ϕ. And as the electron incident energy is increased, the photon will be emitted with an increasing probability in a cone around the electron incident direction,

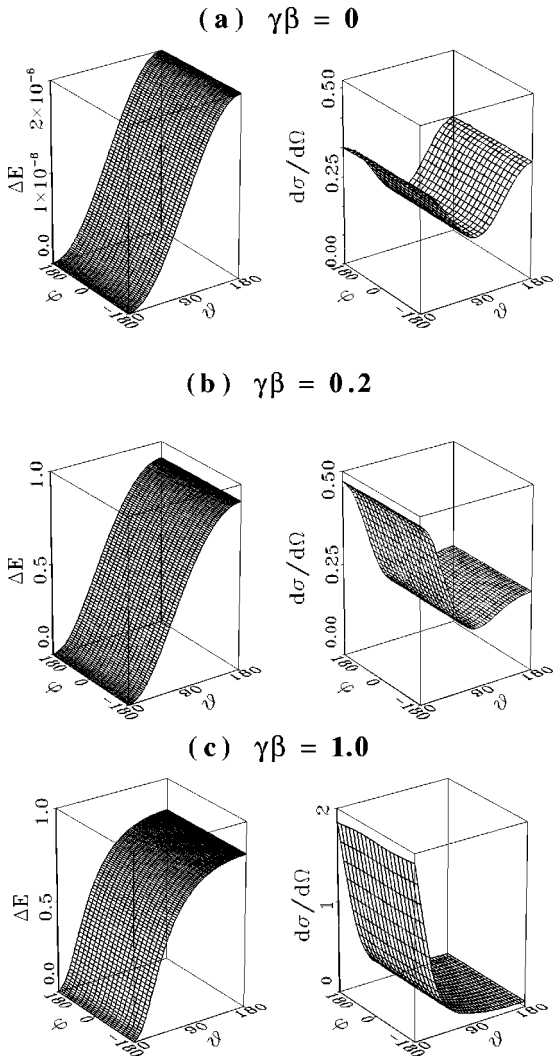

FIG. 2. Differential cross section and energy exchange in the ordinary Compton scattering when the electron is at rest or runs parallel to the photon propagation direction for different electron initial momentum. $\omega/m_e=10^{-6}$ for this and all the following figures.

namely, the forward scattering is enhanced. This phenomenon is very similar to the synchrotron radiation of high-energy electrons, in which most of the emitted photons are confined to a small cone around the electron-beam direction. On the other hand, the energy change $\Delta E/\omega$ reaches maximum when the photon is backscattered ($\theta=180°$). Thus it can be understood that the average energy change in Fig. 3 is

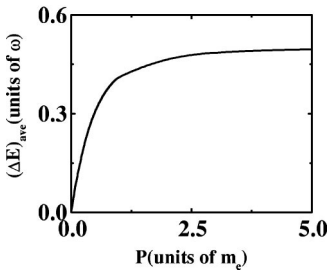

FIG. 3. Variation of the average electron energy change versus its initial momentum in the case of Fig. 2. ΔE is in units of ω and $d\sigma/d\Omega$ is in units of πr_0^2.

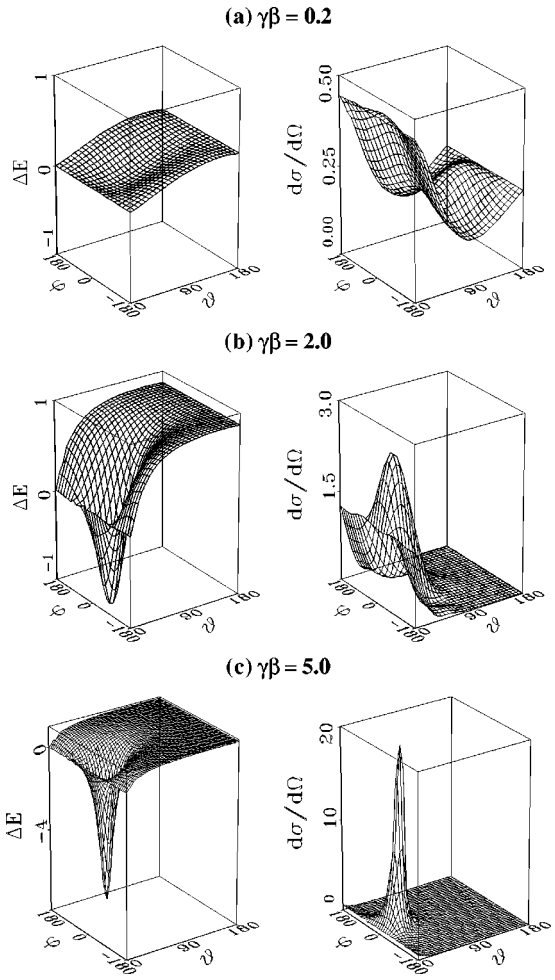

FIG. 4. The same as Fig. 2 but the electron runs with a crossing angle $\alpha=30°$ relative to the photon propagation direction. ΔE is in units of ω and $d\sigma/d\Omega$ in units of πr_0^2.

almost invariant when $\gamma\beta$ is large enough. As already mentioned the electron will never lose energy when $\alpha=0$, viz. $\Delta E\geqslant 0$. It is no wonder that $(\Delta E)_{\text{ave}}\geqslant 0$. But when we turn to the case with $\alpha\neq 0$, things begin to change.

Figures 4 and 5 show the case when $\alpha=30°$. As expected, when $\gamma\beta$ is large enough, the electron energy will be reduced if the photon is scattered into a cone around the incident electron direction with the cone angle α_0' smaller than α, which is quite opposite to those shown in Fig. 2. Correspondingly, for relativistic electrons, the most probable direction of the emitted photon is also in a small crossing angle around **p**. Thus it can be concluded that for high-energy elec-

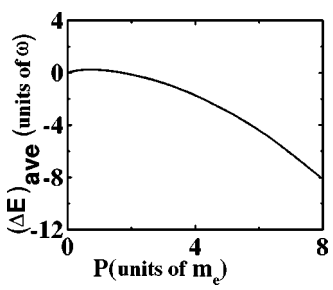

FIG. 5. The same as Fig. 3 but the electron runs with a crossing angle $\alpha=30°$ relative to the photon propagation direction.

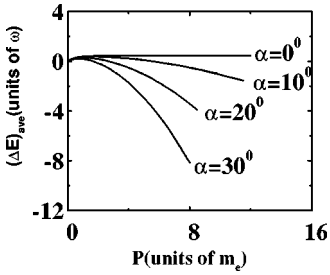

FIG. 6. More examples for the variation of the electron average energy change versus its initial momentum for different crossing angle α in ordinary Compton scattering.

trons the average energy change will be negative. This is really the case as can be seen in Fig. 5. Generally speaking, the sign of $(\Delta E)_{\rm ave}$ is determined by both α and the electron initial energy. Figure 6 shows more examples of the relationship between $(\Delta E)_{\rm ave}$ and $P(=\gamma\beta)$. An interesting phenomenon about Fig. 6 is that for an incident electron with definite energy, there will always exist a delimiting angle α^*; so long as the electron incomes with a crossing angle α less than α^*, it will obtain net average energy gain after the interaction. The smaller the electron initial energy is, the bigger will α^* be. From another viewpoint, the electron loses energy on average so long as its energy is large enough under the condition $\alpha\neq 0$.

All the above results and discussions are based on the ordinary Compton scattering. The nonlinear Compton scattering, which plays a much more important role in the interaction between the free electron and the strong laser field, will be discussed in detail next.

III. NONLINEAR COMPTON SCATTERING

In an intense laser field, a new free-electron–photon interaction mechanism, usually called nonlinear Compton scattering (NLCS), in contrast to the ordinary or linear Compton scattering, emerges. Besides the number of photons involved in the interaction, the other conspicuous characteristic of NLCS is its dependence on the field intensity. When the field intensity is high and the number of photons is large, the electron dynamics, such as the electron energy change and the reaction probability will be much different from those discussed above for ordinary Compton scattering. Similar to Sec. II, we will conduct the study in two steps. First, theoretical formulas used in the calculations will be derived, and next the numerical results and discussions will be presented.

A. Theory

A great deal of theoretical discussion describing the free-electron–photon interaction in a strong laser field appeared in the 1960s [8]. Here we will just give the main points of the widely applied theory [18] before going to the analysis and numerical calculation.

The interaction configuration is the same as that given in Fig. 1 except that k is changed into nk and the electron is dressed by a plane wave $A^\mu=A^\mu(\psi)$, where $\psi=k\cdot x$.

With $p^2=m_e^2$, $k^2=0$, and γ^μ denoting the Dirac matrix, the plane-wave-dressed electron is described by the well-known Volkov state,

$$\Phi_p=\left[1+\frac{e}{k\cdot p}(\gamma\cdot k)(\gamma\cdot A)\right]\frac{e}{\sqrt{2p_0}} \times\exp -i\left\{p\cdot x+\int_0^{k\cdot x}\left[\frac{e}{k\cdot p}p\cdot A-\frac{e^2}{2k\cdot p}A^2\right]d\phi\right\}, \tag{12}$$

which is the solution of the Dirac equation,

$$\gamma^\mu(i\partial_\mu-eA_\mu)\Phi_p=0. \tag{13}$$

When the above dressed state is simultaneously transited from Φ_p to $\Phi_{p'}$, a high-frequency photon having four momentum $k^{\mu'}=(\omega',\mathbf{k}')$ and four-polarization vector ϵ' is emitted. To the first order, the S-matrix element is

$$S_{fi}=-ie\int\overline{\Phi}_{p'}(\gamma\cdot\epsilon^{*\prime})\Phi_p\frac{e^{ik\cdot x}}{\sqrt{2\omega'}}d^4x, \tag{14}$$

from which the reaction cross section can be obtained. For a circularly polarized plane wave,

$$A^\mu=A_{1\mu}\cos\phi+A_{2\mu}\sin\phi, \tag{15}$$

where $(eA_1/m_ec)^2=(eA_2/m_ec)^2=Q^2$ and $A_1\cdot A_2=0$, the differential cross section has a very simple form [18],

$$\frac{d\sigma}{dy}=\sum_n\frac{d\sigma_n}{dy}, \tag{16}$$

where

$$\frac{d\sigma_n}{dy}=\frac{2\pi r_0^2}{x}\left\{-\frac{4}{Q^2}J_n^2(z)+\left(2+\frac{u^2}{1+u}\right)\times[J_{n-1}^2(z)+J_{n+1}^2(z)-2J_n^2(z)]\right\}, \tag{17}$$

in which

$$x=\frac{2k\cdot p}{m_e^2},\quad y=\frac{k\cdot k'}{p\cdot k},\quad u=\frac{y}{1-y},$$
$$z=Q\sqrt{1+Q^2}\,\frac{2}{x}\sqrt{u\left(\frac{nx}{1+Q^2}-u\right)}. \tag{18}$$

The total cross section is

$$\sigma_{n,T}=\frac{2\pi r_0^2}{x}\frac{1}{Q^2}\int_0^{nx/(1+Q^2)}\frac{du}{1+u^2}\left\{-4J_n^2+Q^2\left(2+\frac{u^2}{1+u}\right)\times[J_{n-1}^2+J_{n+1}^2-2J_n^2]\right\}. \tag{19}$$

As $n=1$ and $Q\to 0$, Eqs. (17) and (19) will evolve to Eqs. (2) and (4), respectively [18].

It is often believed that Eq. (17) describes the following nth order NLCS,

$$e+nk\to e'+k' \tag{20}$$

in which the corresponding four-momentum conservation is expressed as

$$q+nk=q'+k', \tag{21}$$

where

$$q=p+\frac{e^2\langle A^2\rangle}{2p\cdot k}k, \tag{22}$$

$$q'=p'+\frac{e^2\langle A^2\rangle}{2p'\cdot k}k \tag{23}$$

are the so-called quasimomenta of the electron embedded in the plane wave.

From Eq. (21), we can get the frequency of the scattered photon and the electron energy change,

$$\left(\frac{\omega'}{\omega}\right)=n\frac{\gamma(1-\beta\cos\alpha)}{\gamma(1-\beta\cos\alpha')+\{n\omega/m_e+Q^2/[2\gamma(1-\beta\cos\alpha)]\}(1-\cos\theta)}, \tag{24}$$

$$\left(\frac{\Delta E}{\omega}\right)_n=n-\frac{\omega'}{\omega}\left\{1+\frac{Q^2}{2}\frac{1-\cos\theta}{\gamma(1-\beta\cos\alpha)[\gamma(1-\beta\cos\alpha)-\omega'/m_e(1-\cos\theta)]}\right\}. \tag{25}$$

The subscript n represents the n-photon-absorption reaction.

To acquire the average electron energy change $(\Delta E)_{\mathrm{ave},n}$, the relationship between dy and $d\Omega'$ must be known first. For this purpose, we return to the electron's rest frame, in which

$$y=\frac{\omega\omega'}{p\cdot k}(1-\cos\theta)$$

$$=\frac{\omega}{p\cdot k}n\omega\frac{1-\cos\theta}{1+(n\omega/m+Q^2/2)(1-\cos\theta)}. \tag{26}$$

Thus,

$$\frac{dy}{d\cos\theta}=\frac{\omega'^2}{np\cdot k}. \tag{27}$$

Because the whole dynamics is symmetric with respect to ϕ in this frame, hence

$$dy=\frac{dy}{d\Omega'}d\Omega'=\frac{\omega'^2\,d\Omega'}{2\pi np\cdot k}. \tag{28}$$

Because $\omega'^2\,d\Omega'$ is Lorentz invariant, the expression for $(\Delta E)_{\mathrm{ave},n}$ in the laboratory frame can be obtained,

$$\left(\frac{\Delta E}{\omega}\right)_{\mathrm{ave},n}=\frac{\int(d\sigma_n/dy)(\Delta E/\omega)(dy/d\Omega')d\Omega'}{\sigma_{n,T}}. \tag{29}$$

It is expected that the dependence on n and Q of $(\Delta E/\omega)_{\mathrm{ave},n}$ will make the energy exchange characteristics in NLCS quite different from that of the ordinary Compton scattering.

B. Numerical results and discussion

Before discussing the characteristics of the energy exchange in NLCS, we shall first present the analysis of the high-frequency-photon emission through Eq. (18).

Figure 7 shows the dependence of $\sigma_{n,T}$ on the initial condition represented by $x=2p\cdot k/m_e^2=2\gamma(1-\beta\cos\alpha)\omega/m_e$, which is proportional to the photon frequency in the electron's rest frame. It is important to note that the reaction probability of nth order NLCS is not sensitive to the initial conditions in a wide range of x. For example, when the 46.6-GeV e beam from SLAC is used in the head-on collision with Nd: glass laser pulses [14], x is below 0.8. In a typical electron inelastic scattering by intense continuous laser beam with $Q<10$, one gets $x<10^{-4}$. Because ω/m_e has been set to 10^{-6}, x is decided by the electron initial energy and its incoming angle θ. The results obtained as shown in Fig. 7 tell us the total nth order reaction probability does not change very much whether the electron is incident along or against the photon propagation direction, viz., $\sigma_{n,T}$ is decided mainly by the order n and the field intensity Q.

The dependence of $\sigma_{n,T}$ on Q and n makes NLCS quite different from ordinary Compton scattering with $Q=0$ and $n=1$. The relationship between $\sigma_{n,T}$ and Q for different n is shown in Fig. 8, where it can be seen easily that as Q in-

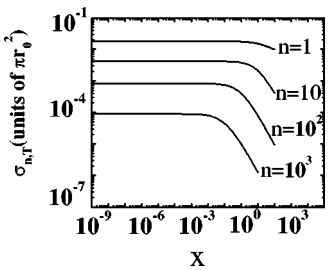

FIG. 7. The dependence of the total cross section σ_{nT} on the initial conditions denoted by $x=2p\cdot k/m_e^2$ of the laser-electron interaction for different order n in the nonlinear Compton scattering.

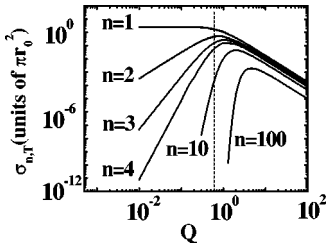

FIG. 8. The field-intensity dependence of the total cross section for the nth order nonlinear Compton scattering. The dotted line corresponds to the laser intensity $Q=0.6$, which is the value used in Bula's experiment.

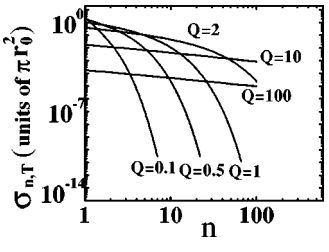

FIG. 9. The total cross section of nth-order nonlinear Compton scattering as a function of n for different field intensities.

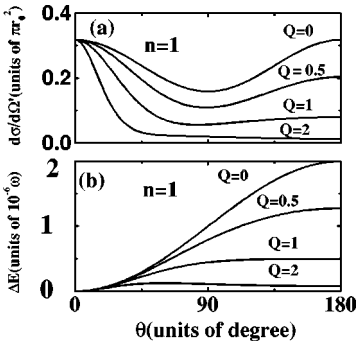

FIG. 10. The differential cross section and electron energy change as a function of θ for different field intensities in the nonlinear Compton scattering with $n=1$. The line with $Q=0$ corresponds to the ordinary Compton scattering. The electron is initially at rest. Because the whole system is symmetric with respect to the azimuthal angle ϕ, the dependence upon ϕ is omitted.

creases the contribution of high-order NLCS to laser–free-electron interaction will become more and more important. For $Q>0.1$, the importance of NLCS with $n\geqslant 2$ begins to emerge. Then, after a transition region from $Q=0.1$ to $Q=10$, the NLCS contribution becomes prominent compared with that of the ordinary Compton scattering. It can be said that when $Q>10$, NLCS will dominate the laser–free-electron interaction. Furthermore, it is worthwhile pointing out that the above thresholds $Q=0.1$ and $Q=10$ are consistent with the results found in the research of the inelastic electron scattering by a stationary laser beam. The results showed that the inelastic effect begins to appear as $Q>0.1$ and becomes dominant as $Q>10$. Hence, from the above discussions, we have another reason to attribute the inelastic effect in the intense-laser–free-electron scattering to NLCS. Moreover, besides the appearance of high-order NLCS, Fig. 8 shows us that the low-order NLCS will be suppressed as Q increases further. For example, when $n=10$, $\sigma_{n,T}$ will increase with Q until $Q\sim 10$. Then as the field intensity becomes higher, $\sigma_{n,T}$ begins to decrease while the contribution from higher-order NLCS, such as $n=100$, 200, etc. becomes again more and more important. Actually, when $Q\rightarrow 0$, the increasing part of the curves in Fig. 8 is proportional of $Q^{2n-2}(n\geqslant 1)$, which can be estimated from Eq. (17) by using $J_n(z)\propto Q^n$. Moreover, when Q is large enough, viz., in the decreasing part of the corresponding curves in Fig. 8, $\sigma_{n,T}\propto 1/Q^2$. By numerical analysis, we find that the two scaling laws are fully consistent with Fig. 8. Hence, it can be said that as the field intensity Q is being increased, the nth order total cross section $\sigma_{n,T}$ will first increase rapidly, especially when n is large, and will then decrease at a much slower rate after reaching maximum.

Recently, Bula *et al.* [14] has performed the experiment on NLCS at $Q=0.6$. According to Fig. 8, it can be found that the total reaction probability with $n>10$ is smaller than that with $n=4$ by several orders. This is consistent with the experimental results quantitatively, which has demonstrated the reaction order up to $n=4$.

From another viewpoint, the above results can also be found in Fig. 9, which shows the relationship between $\sigma_{n,T}$ and n for different Q. For definite Q, $\sigma_{n,T}$ decreases with n. And when $Q<1$, the cross section drops rapidly where as $Q>10$, it varies smoothly, firmly demonstrating the importance of the high-order NLCS.

Up to now, we have put the emphasis upon the importance of high-order NLCS. Since the electron inelastic scattering is directly related to the electron energy exchange, it is natural to ask what are the energy exchange characteristics in NLCS.

To compare with the case of the ordinary Compton scattering, we first consider the differential cross section and the energy change with $n=1$ and $\alpha=0$. As shown in Fig. 10, when Q increases both the reaction cross section and the energy exchange will be reduced, namely the low-order reaction (here $n=1$) will be suppressed in high-intensity fields. This can be explained using a simplified physical picture. With the field intensity increasing, the electron drift velocity and effective mass m_e^* will be increased too. Thus, for high intensity laser fields, the sharp peaking of the differential cross section in the forward direction in Fig. 10(a) is very similar to that in Fig. 2 for ordinary Compton scattering with increasing electron velocity. Similarly, the decreasing of energy changes with increasing Q in Fig. 10(b) can be attributed to the increased effective mass m^*. Of course, the above analog does not mean an exact account can be given since the interaction mechanisms are in essence quite different. When $\alpha\neq 0$, the conclusion found in Fig. 10 can be seen to be true also in Fig. 11 with $\alpha=30°$. Compared with Fig. 4(c), which has the same electron energy and electron/photon crossing angle ($=30°$), both $(d\sigma_{nT}/d\Omega)$ and $\Delta E/\omega$ are suppressed as Q increases although the forward scattering of the photon is similar [20].

For high-order NLCS, the differential cross section is quite different, as shown in Fig. 12. It is obvious that the contribution to forward scattering ($\theta=0$) is mainly from the $n=1$ reaction. And when the initial velocity of the electron running along the incident photon is increased, the influence of the relativistic effect upon NLCS is more pronounced, viz., the scattered photons is limited to a smaller and smaller solid angle with an increasing probability. This phenomenon is very similar to the harmonic production by the electron embedding in a plane wave in the classical electrodynamics.

The overall contribution from high-order NLCS ($n\geqslant 2$) to the total cross section and average energy exchange can be expressed as

$$\sigma_{n\geqslant 2,T}=\sum_{n=2}^{+\infty}\sigma_{n,T}, \tag{30}$$

$$\left(\frac{\Delta E}{\omega}\right)_{n\geqslant 2,T}=\frac{\sum_{n=2}^{+\infty}(\Delta E/\omega)_{\mathrm{ave},n}\sigma_{n,T}}{\sum_{n=1}^{+\infty}\sigma_{n,T}}. \tag{31}$$

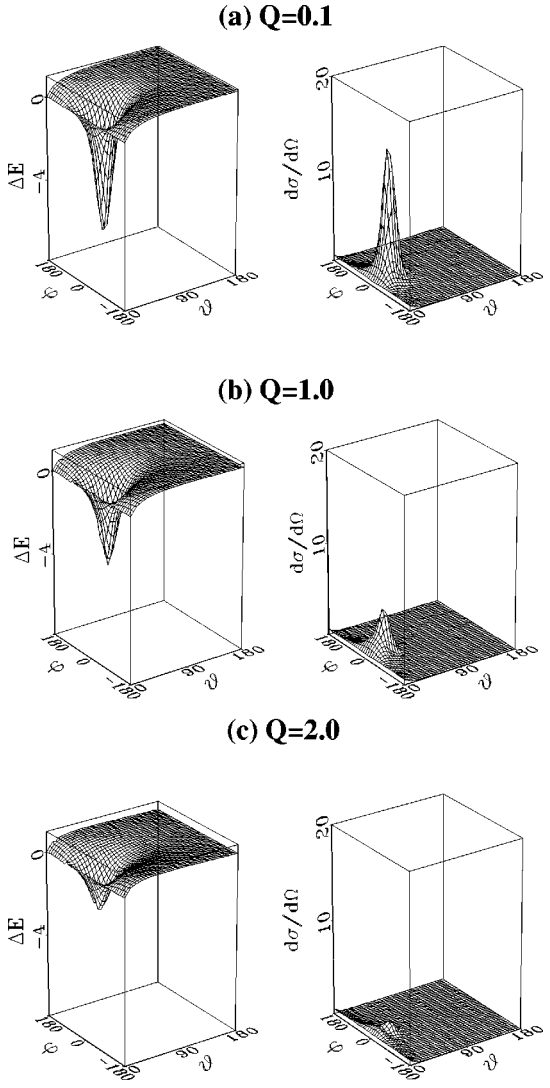

FIG. 11. The same as in Fig. 10 but the electron runs with a cross angle $\alpha=30°$ relative to the photon propagation direction and an initial momentum $|\mathbf{p}|=5m_e$. ΔE is in the units of ω and $d\sigma/d\Omega$ is in the units of πr_0^2.

Figure 13 shows the dependence of $\sigma_{n\geqslant 2,T}$ and $(\Delta E/\omega)_{n\geqslant 2,T}$ on the field intensity when the electron is at rest. For comparison, the case with $n=1$ is also presented and $(\Delta E/\omega)_{1,T}$ is defined as

$$\left(\frac{\Delta E}{\omega}\right)_{1,T}=\frac{(\Delta E/\omega)_{\mathrm{ave},1}\sigma_{1,T}}{\Sigma_{n=1}^{+\infty}\sigma_{n,T}}. \tag{32}$$

It is marvelous to notice that as Q increases, the NLCS with $n\geqslant 2$ plays a more and more important role in both the average energy exchange and the total reaction probability while the reaction with $n=1$ is greatly suppressed. The positive sign of the average energy exchange is the same in the NLCS as well as in ordinary Compton scattering when the electron is at rest, which can be easily understood. When we turn to the conditions with $\alpha\neq 0$, as is shown in Fig. 13, the above conclusions remain the same except that the average electron energy exchange is negative when the electron energy is large enough, which is similar to the ordinary Compton scattering. It should be mentioned that Figs. 13(b) and 14(b) are almost the same, which demonstrate once more the insensitivity of the cross section $\sigma_{n,T}$ to the initial conditions as has been shown in Fig. 7.

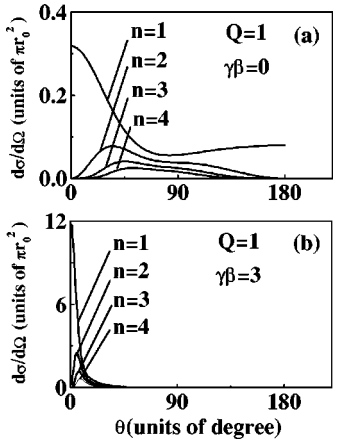

FIG. 12. Differential cross section of NLCS with $n=1,2,3,4$ for different electron initial momentum: (a) $\gamma\beta=0$ and (b) $\gamma\beta=3$. The electron is incident along the photon propagation direction with $\alpha=0$.

From all the above numerical results and discussions about NLCS, we can see that the most significant characteristics of NLCS is the important role played by the high-order reactions in affecting both the average electron energy exchange and the total reaction probability when the intense laser field is used.

IV. SUMMARY

In this paper, we have studied numerically in detail the energy exchange characteristics in the ordinary Compton scattering and NLCS. The main conclusions can be summarized as follows:

(1) When the electron runs parallel to the photon propa-

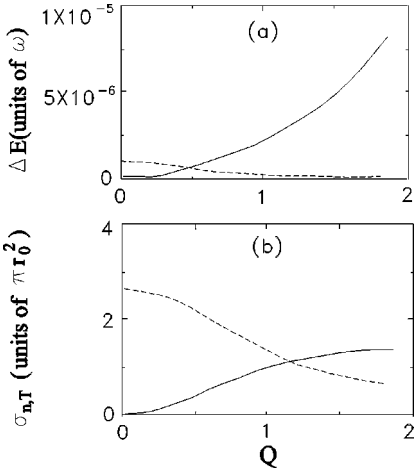

FIG. 13. A comparison of the contributions from the nonlinear Compton scattering with $n=1$ (dotted line) and $n\geqslant 2$ (solid line) to the average electron energy change and the total cross section of the laser–electron interaction as a function of the field intensity Q. The electron is at rest initially.

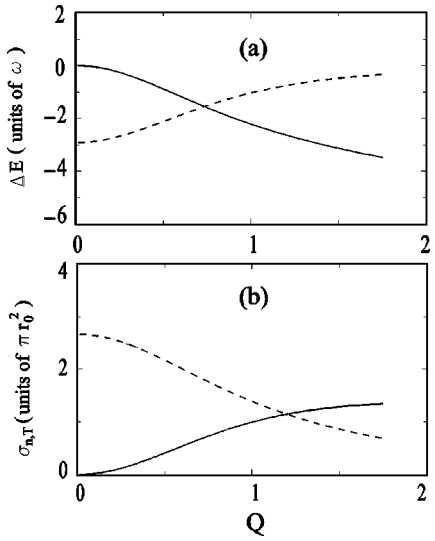

FIG. 14. The same as in Fig. 12 but the electron runs with a crossing angle $\alpha=30°$ relative to the photon propagation direction and an initial momentum $|\mathbf{p}|=5m_e$.

gation direction or its energy is low enough with arbitrary crossing angle ($0<\alpha<180$), its average energy change will be positive. On the other hand, for the electron with energy large enough, it will lose energy on the average for $\alpha\neq 0$. This result will help to design the electron acceleration by intense lasers in vacuum.

(2) When the field intensity is low ($Q\ll 1$), the mechanism of the free-electron–laser interaction is mainly the ordinary Compton scattering, and when $Q>0.1$, the importance of NLCS begins to show. And for $Q>10$, NLCS will dominate the interaction. Using this conclusion, we can explain the intensity-threshold effect found in the study of electron inelastic scatterings by an intense stationary laser beam.

(3) When the field intensity increases, the low-order NLCS will be suppressed and high-order NLCS will play a more important role, resulting in much greater energy exchange and total reaction probability. This is not only consistent with electron radiation studies in the classical framework, but also consistent with the results obtained in our other paper [21], which states that as $Q\gtrsim 100$, the electron can be captured and get violent acceleration by the laser beam. It is hoped that these conclusions can be submitted to the NLCS experimental test.

ACKNOWLEDGMENTS

The authors wish to thank Professor C. M. Fou for a carefully reading this manuscript and for enlightening discussions. This work was partially supported by the National Natural Science Foundation of China, under Contract No. 19684001, the National High-Tech ICP Committee in China, and the Science and Technology Funds of China.

[1] R. R. Freeman, T. J. McIlrach, P. H. Busksbaum, and M. Bashkansky, Phys. Rev. Lett. **57**, 3156 (1986).
[2] H. G. Muller, A. Tip, and M. J. van der Wiel, J. Phys. B **16**, L679 (1983).
[3] M. H. Mittleman, Phys. Rev. A **29**, 2245 (1984).
[4] K. Kulander and A. L'Huillier, J. Opt. Soc. Am. B **7**, 403 (1990), and references therein.
[5] P. Sprangle, E. Esarey, and A. Ting, Phys. Rev. Lett. **64**, 2011 (1990).
[6] T. Katsouleas and J. M. Dawson, Phys. Rev. Lett. **51**, 392 (1983).
[7] T. C. Katsouleas, Proc. SPIE **664**, 2 (1986), and references therein.
[8] T. W. Kibble, Phys. Rev. **138**, B740 (1965); L. M. Franz, *ibid.* **139**, B1326 (1965).
[9] A. I. Nikishov and V. I. Ritus, Sov. Phys. JETP **19**, 1191 (1964); L. V. Keldysh, **10**, 1309 (1965).
[10] F. Ehlotzky, Can. J. Phys. **63**, 907 (1985), and references therein.
[11] Vachaspati, Phys. Rev. **128**, 664 (1962); E. S. Sarachik and G. T. Schappert, Phys. Rev. D **1**, 2738 (1970); F. V. Hartemann and A. K. Kerman, Phys. Rev. Lett. **76**, 624 (1996).
[12] K. T. McDonald, in *Laser Acceleration of Particles*, edited by Chan Joshi and Thomas Katsouleas, AIP Conf. Proc. No. 130 (AIP, New York, 1985), p. 23.
[13] K. T. McDonald, P. Chen, J. E. Spencer, and R. B. Palmer, in *Proceedings of the Workshop on Beam-Beam and Beam-Radiation Interactions-High Intensity and Non-linear Effects* (World Scientific, Singapore, 1992), p. 127.
[14] C. Bula *et al.*, Phys. Rev. Lett. **76**, 3116 (1996).
[15] Y. K. Ho, J. X. Wang, L. Feng, W. Scheid, and H. Hora, Phys. Lett. A **220**, 189 (1996).
[16] J. X. Wang, Y. K. Ho, and W. Scheid, Phys. Lett. A **231**, 139 (1997).
[17] J. X. Wang, Y. K. Ho, and W. Scheid, Phys. Lett. A **234**, 415 (1997).
[18] V. B. Berestetskii, E. M. Lifshitz, and L. P. Pitaevskii, in *Quantum Electrodynamics*, Course of Theoretical Physics, 2nd ed., translated from Russian by T. B. Sykes and J. S. Bell (Pergamon, New York, 1982), Vol. 4, pp. 118, 354, 449.
[19] T. W. B. Kibble, Phys. Rev. Lett. **16**, 1054 (1966); Phys. Rev. **150**, 1060 (1966).
[20] Y. I. Salamin and F. H. M. Faisal, Phys. Rev. A **54**, 4383 (1996).
[21] J. X. Wang, Y. K. Ho, Q. Kong, L. J. Zhu, L. Feng, S. Scheid, and H. Hora, Phys. Rev. E **58**, 6575 (1998).